SF2A 2021
A. Siebert, K. Baillié, E. Lagadec, N. Lagarde, J. Malzac, J.-B. Marquette, M. N'Diaye, J. Richard, O. Venot (eds)

THE HI-5 NULLING INSTRUMENT AND SCIFYSIM: AN END-TO-END SIMULATOR FOR INTEGRATED OPTICS BEAM COMBINERS

R. Laugier[1], D. Defrère[1] and A. Bigioli[1]

Abstract. By limiting the precision of the fringe visibility measurement, photon noise is a major obstacle to the capability of interferometers to detect exoplanets at the smallest angular separations. To circumvent this limitation, the SCIFY project aims to design, build and commission Hi-5: the first nulling instrument for the VLTI, operating in the L' band, a sweet spot for the detection of young giant exoplanets. Based on an integrated optics chip combining all four VLTI beams into a double Bracewell configuration, it will enable medium spectral resolution (R=2000) in the L' band of giant exoplanets between 5 and 50 mas from their star. The end-to-end simulator SCIFYsim is being developed to predict the performance of this new instrument in the presence of a wide variety of instrumental errors, like optical path difference residuals from fringe tracking, wavefront error at the injection, longitudinal dispersion, chromaticity of the combiner chip, and more. As it was designed for modularity, this simulator could also be used to study the performance of other types of integrated beam combiners operating in realistic conditions, like ABCD pairwise combiners, or the more elaborate kernel-nulling combiner envisioned for the VIKiNG project. I will present both the current state of the design of the high-contrast combiner Hi-5, and some of the features and early results of SCIFYsim.

Keywords: High contrast, nulling interferometry, long-baseline interferometry, simulations

1 The Hi-5 instrument

Hi-5 is a possible future visitor instrument for the VLTI led by the Institute of Astronomy of KU Leuven and mainly financed by the ERC project SCIFY. Its design is optimized for high contrast observation and the detection and characterization of young giant planets around nearby stars. It will leverage the long baselines of the observatory to do this down to unprecedented angular separations (5 to 50 mas) from their host stars. This challenging observing task can be achieved using nulling interferometry (Bracewell 1978) to work in a regime comparable to coronagraphy where on-axis light is treated in a special way, so that the corresponding photon noise does not affect significantly the scientific measurement.

Hi-5 will offer a spectral resolution of up to $R \approx 2000$ in the L' band (a sweet spot for the direct detection of young giant planets). It should probe uncharted territories in planet formation into shorter orbital period planets, inside the snow line of their system. It should also allow the detection and characterization of some giant exoplanets detected by radial velocity measurements.

The instrument will take advantage of the spatial filtering, stability, and compactness offered by single-mode waveguide integrated (i.e. photonics) beam-combiners, to implement one of the more recent and more complex beam-combiner architectures called Double Bracewell or Angel & Woolf, from the seminal paper (Angel & Woolf 1997). Future evolutions are already considered to leverage more advanced nulling techniques (Martinache & Ireland 2018), that are beyond the scope of current simulation tools (Den Hartog et al. 2003; Absil et al. 2006).

Much like a coronagraph, the performance of a nulling combiner is directly affected by the quality of the wavefront that feeds it. Therefore, predicting its performance requires, in addition to the simulation of the beam-combination device, the simulation of the adverse effects introduced — or partially corrected — by the interferometer's infrastructure and environment, which will be listed in section 3. SCIFYsim is the python-based end-to-end simulator designed to reproduce the complicated interactions between the beam combiner architecture and the various instrumental effects. While Hi-5 is currently in its design phase, the end-to-end simulator, here presented, stands as a guideline to determine and optimize the attainable performances and to provide a working ground for developing data reduction algorithms.

[1] Institute of Astronomy, KU Leuven, Celestijnenlaan 200D, 3001 Leuven, Belgium

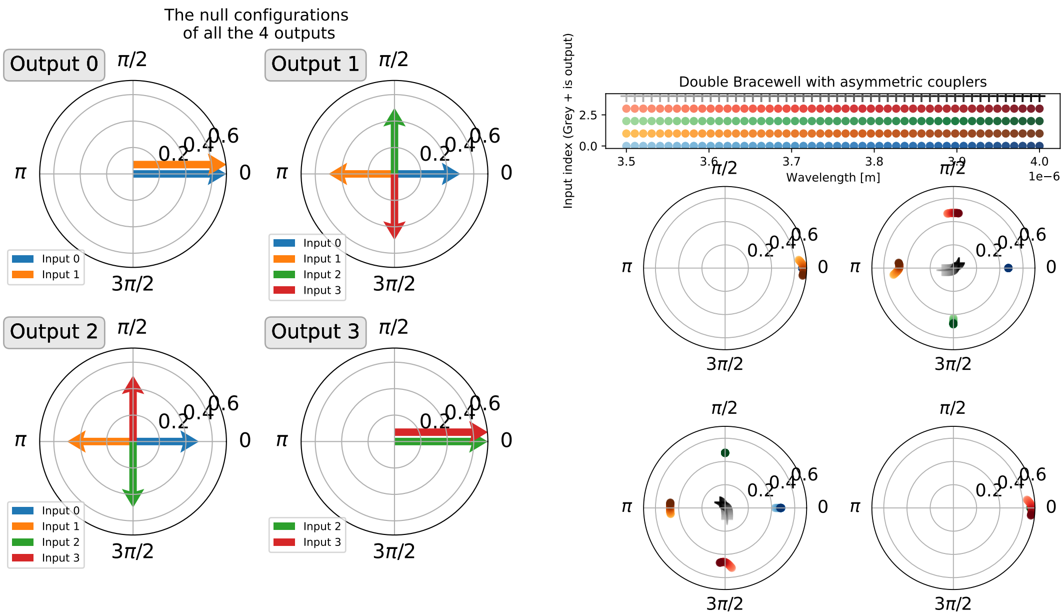

Fig. 1. Left: Graphical representation of achromatic combiner matrix. Right: representation of a chromatic combiner. Each row of the matrix corresponds to an output and is plotted on one complex plane graph. Each column of the matrix corresponds to an input and is plotted in a different color. Each wavelength channel is mapped to a luminance in the color scales. The outputs corresponding to cophased input are plotted in gray tones and its closeness to zero can informs us on the depth of the null.

2 Beam combination

The data flow in SCIFYsim is built around the beam combiner, which is implemented as the matrix of the complex amplitude transfer function of the photonics component. This matrix represents the transformation of the vector of complex amplitude injected into the input waveguides into the vector of complex amplitudes at the outputs.

The spectrograph module then computes the output intensity which is convolved with the spectroscopic PSF to generate the image on the pixels of the detector. The preliminary simulations bypass this step and assume that each wavelength channel is evenly distributed on a fixed number of pixels.

The sensor module computes the integration of light on each pixel, and incorporates readout noise, photon noise, and excess noise in the case of amplified sensors.

3 Aberrations

The main aberrations on the complex amplitude of the injected light are simulated through three independent processes detailed below.

First, for the injection, we assume that the effect of the atmospheric turbulence corrected by an adaptive optics system. The injection is in this case simulated independently for each telescope, using a sliding phase screen based on a spatially filtered Kolmogorov function. Figure 2 shows the simulation of this phasor at three wavelengths which is then interpolated at each spectral channel.

Secondly the simulation of the fringe-tracking residuals is based on a random time series generated on the basis of the temporal power spectrum of optical path differences (OPD) residual measurements taken with the GRAVITY fringe tracker.

Finally, the chromatic component of the OPD errors, arising from the correction of optical paths in delay lines that have different chromatic optical properties from the path atmosphere is split into two components. A static contribution depends on the pointing of the instrument and atmospheric conditions, will be corrected with variable thickness ZnSe plates. Another is dynamic, (called water vapor seeing) will be implemented in the same way as the geometric OPD as it can be measured with the GRAVITY fringe tracker. Both these

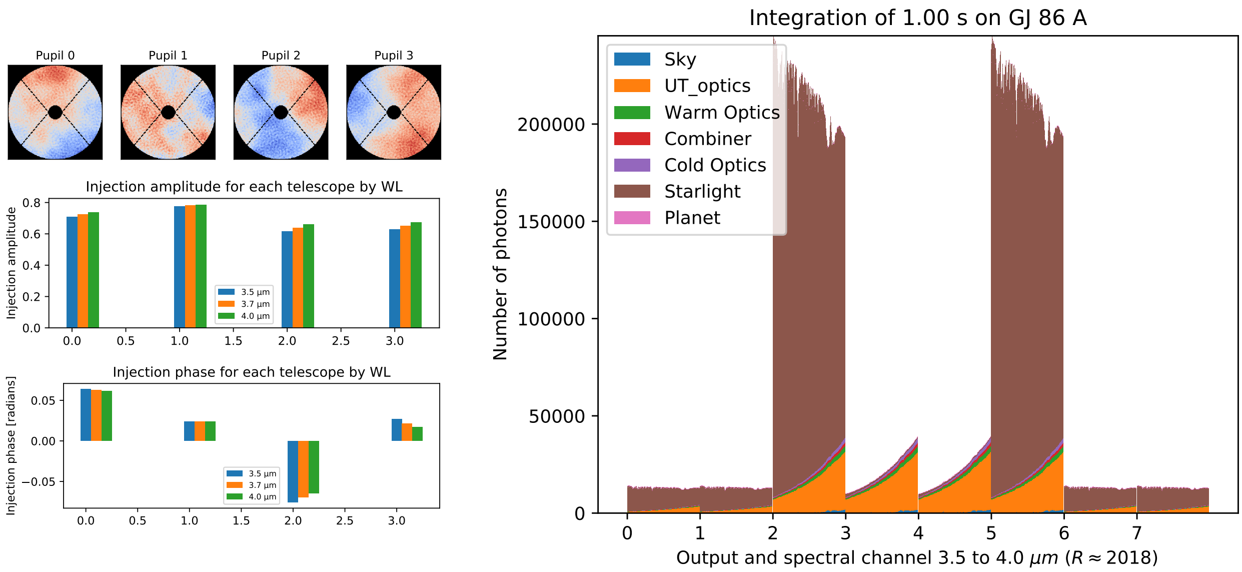

Fig. 2. Left: Detail of the simulation of the injection effect showing the pupil wavefront, and the resulting complex amplitude injected in different wavelength channels in amplitude and phase. The wavefronts are spatially filtered to emulate the effect of the adaptive optics system. **Right:** The decomposition of the (cumulative) contribution of each sources to the different outputs. Within each output, each of the 270 wavelength channel is represented side-by-side, increasing wavelength from left to right. The signal of interest on the two dark channels (3 and 4) is dwarfed by the main contributor: the UT thermal background.

chromatic effects are not considered for the results shown here.

The simulation includes a module simulating transmission and emission in a recursive chain including the sky, the coudé train, the warm optics, the combiner, and the cold optics. They feature a temperature, and a transmission law that is used to infer on the emissivity. If needed, all these sources can be propagated independently to obtain the detail of the contributions to the signal and background for each wavelength channel, as shown in Fig. 2.

Although polarization is not modeled vectorially in the simulator, we consider that the phase mismatch due to the chip birefringence is compensated a the inputs and the polarizations are split in the spectrograph (thus using twice the number of pixels), and we scale the signal accordingly.

4 Early results

The signal of interest produced in the differential output by an off-axis source is shown in Fig. 3. It is shown here as a broadband combination (the instrument will actually work independently in all wavelengths) and takes into account both the radial profile of the injection and the projection of the baselines for a target at a declination of $-50°$ near the meridian. As expected with the combination architecture, the fundamental pattern is the same as could be seen if Fig. 7 of Martinache & Ireland (2018). Depending on the order in which the telescopes are fed into the instrument, either of the three patterns can be chosen.

We use the simulator to generate a series of 100 DIT realizations to evaluate the leakage light and the standard deviation of instrumental noise as a function of the star's magnitude. Noise is then computed as the quadratic sum of the detector readout noise, the photon noise from thermal background and leakage light, and the instrumental noise. It is then adjusted by the number of pixels involved in the reading and the number of DIT used in an integration time.

The signal to noise ratio (S/N) can then be evaluated, assuming a certain position on the map, for any value of star and planet parameters. Here we chose to examine the mean S/R over the 270 spectral channels, therefore our capacity for spectral characterization of the target. An example is shown in Fig. 3 where two regimes can be identified. For bright stars, the noise is dominated by the instrumental noise and the temporal variability of the leakage light, especially at shorter wavelengths. For fainter stars, the noise is dominated by

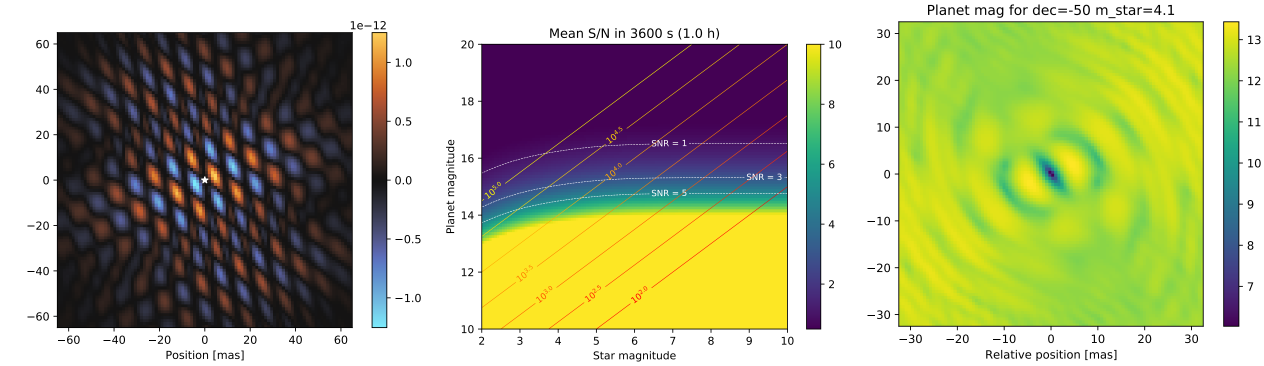

Fig. 3. Left: the broadband ($3.5 - 4\mu$m differential map of one considered configuration observing at declination -50deg. Units are arbitrary, and the optical axis is marked by a white star. While the fundamental pattern visible around the center would repeat to infinity, it is here limited in extent both by the transmission of the fiber injection, and by the bandwidth that produces a radial smearing. **Center:** the mean value of S/N in each spectral channel as a function of star and planet magnitude in the most sensitive region of the map. Diagonal lines indicate the corresponding contrast. **Right:** the sensitivity map around a magnitude 4.1 star. Combining the different wavelengths and pointings produces a smoothing of the sensitivity regions.

the thermal background of the optical train, especially at longer wavelengths.

In order to compute the detection performance, we follow the example given by Ceau et al. (2019) and establish a T_E test of detection. This test, while not the most powerful, provides realistic performance prediction in rejecting the null hypothesis (of the absence of detectable features) for an unknown detected signature. Here, we use a numerical approach to invert the P_{Det} function and obtain the magnitude of the fainter single planet that would be detected with a probability of 90%

These results are a first approximation as the figures for the input aberrations are not yet representative, and some features of the simulator are yet to be implemented.

5 Conclusion

Hi-5 will pioneer L-band photonics instruments and be the first to use photonics to deploy one of the advanced nulling architecture at a long-baseline interferometric facility. Details of the design, the performance evaluation, and yield estimation are in progress and will be described in coming peer-reviewed publications.

The simulator SCIFYsim was designed for flexibility. As it is articulated around the complex amplitude transfer matrix of arbitrary single mode photonic device with its output sent into a spectrograph, it can just as easily be used to simulate the behavior of instruments like GRAVITY, PIONIER, or even monolithic aperture devices like GLINT, opening the door to more complex architectures like VIKiNG (Martinache & Ireland 2018).

SCIFY has received funding from the European Research Council (ERC) under the European Union's Horizon 2020 research and innovation program (grant agreement No 866070).

References

Absil, O., Hartog, R. D., Gondoin, P., et al. 2006, 800, 787

Angel, J. R. P. & Woolf, N. J. 1997, The Astrophysical Journal, 475, 373

Bracewell, R. N. 1978, Nature, 274, 780

Ceau, A., Mary, D., Greenbaum, A., et al. 2019, Astronomy and Astrophysics, 630, 1

Den Hartog, R., Absil, O., Kaltenegger, L., et al. 2003, European Space Agency, (Special Publication) ESA SP, 399

Martinache, F. & Ireland, M. J. 2018, Astronomy and Astrophysics, 619, 1